

One Step One Pot Mechano-synthesis of Boron Doped Titanium Nitride and its Microstructure Characterization.

Ujjwal Kumar Bhaskar

Department of Physics, Sreegopal Banerjee College, Bagati, Magra, Hooghly-712148, India.

Email: ukb1975@yahoo.com

Abstract- The boron doped nanostructured titanium nitride ($Ti_{0.9}B_{0.1}N$) has been synthesized ball-milling the stoichiometric powder mixture of α -Ti and boron in desired molar ratio, under nitrogen atmosphere at room temperature. After one hour of milling it is observed that a part of α -Ti phase converted into metastable β -Ti (cubic) phase and survives up to 3h of milling. The stoichiometric $Ti_{0.9}B_{0.1}N$ (cubic) phase is initiated after 1h of milling and formed completely after 7h of milling. Microstructure characterizations of unmilled and all ball-milled powders are made by analyzing their respective X-ray diffraction (XRD) patterns employing the Rietveld structure and microstructure refinement method. Inclusion of B and nitrogen atoms in the compound has been confirmed by energy dispersive X-ray (EDX) analysis and from the comparative study of lattice parameter variations of TiN and $Ti_{0.9}B_{0.1}N$. Microstructure characterization of the prepared samples done by transmission electron microscopy (TEM) reveals that average size of almost monodispersed spherical particles of $Ti_{0.9}B_{0.1}N$ is ~ 5 nm which is in good agreement with the Rietveld analysis.

Index Terms- Ball-milling; Microstructure; X-ray diffraction; HRTEM; Phase transition.

1. INTRODUCTION

In the last four decades, titanium based metal nitride protective coatings have been used in many applications due to their excellent wear, erosion, and corrosion resistance [1–4]. The addition of boron was found to enhance the high temperature stability, good corrosion and wear resistance of these hard coating materials [5, 6].

In the present study we have prepared single phase nanocrystalline TiBN powder by using mechanical alloying (MA). The room temperature synthesis of single phase nanocrystalline TiBN powder in single step through this route has not been reported yet. Mechanical alloying or ball-milling is the simple route to synthesize nanocrystalline materials in large scale. The ball-milling methods to synthesize the nanostructure materials have the number of advantages: i) It is a single step single pot method, ii) It does not involve sophisticated instruments and harmful chemicals, iii) Tailor made nano structured materials are synthesized with in very short duration of time [7].

The objective of the present work are to prepare nano-structured TiBN phase out of elemental powder materials and to characterize the microstructure of prepared materials by Rietveld analysis and from HRTEM analysis and to correlate the results of both the analysis.

2. EXPERIMENTALS

Precisely weighted 0.9 mole fraction of α -Ti powder (Alfa Aesar, 300 mesh, purity 99.5%) and 0.1 mol fraction of fine boron powders was ball milled under N_2 atmosphere at room temperature in a planetary ball mill (Model P5, M/S Fritsch, GmbH, Germany) using a pot of 80cc volume with 30 chrome steel balls of 1cm diameter. The ball to powder mass ratio was taken 30:1 and the rotational speed of planetary ball-mill was optimized at 300rpm. The planetary ball-mill was performed for different milling duration from 1h to 9h.

The X-ray powder diffraction patterns of the prepared powder materials were recorded in step scan (step size $0.02^\circ 2\theta$; counting time 5–10 s/step) mode using Ni-filtered CuK_α radiation from a highly stabilized and automated Philips X-ray generator (PW1830) operated at 40 kV and 20mA.

The SEAD and HRTEM images were taken by TEM (FEI, Tecnai G² F30-ST operated at 300 kV) equipped with a Gatan Oriels CCD camera.

3. METHOD OF ANALYSIS

The Rietveld's powder structure refinement method was adopted to analyze the XRD patterns of the prepared sample by using specially designed Rietveld's software MAUD [8–16]. The output of the analysis gives the refined data for structure parameters

in terms of atomic coordinates, occupancies, lattice parameters, thermal parameters, etc. and microstructure parameters such as particle size, r.m.s. lattice strain and stacking fault probability. The calculated XRD patterns of unmilled and all ball-milled samples are simulated considering the presence of boron (trigonal, sp. gr. R-3m:H, $a = 0.3854531$ nm, $c = 1.2506178$ nm), α -Ti (hcp, sp. gr. P6₃/mmc, $a = 0.29445$ nm $c = 0.4679$ nm), β -Ti (bcc, sp. gr. Im-3m, $a = 0.33202$ nm), and $\text{Ti}_{0.9}\text{B}_{0.1}\text{N}$ (fcc, sp. gr. Fm-3m, $a = 0.42322$ nm) phases including diffraction optics effects, instrumental factors and other specimen characteristics. The refinement process continues until the best fitting is obtained with the value of Goodness of fitting (GoF) very close to unity. The back ground intensity of all XRD patterns were fitted by a polynomial of degree 5. The peak shape is assumed to be a pseudo-Voigt (pV) [8, 9, 14-16] type profile.

4. RESULTS AND DISCUSSION

4.1. Nanostructure characterization by XRD

XRD patterns of all ball-milled and unmilled samples are shown in Fig.1. The unmilled (0h) XRD pattern consists of reflections of α -Ti (hcp) (ICSD# 52522) and boron (ICSD# 56992) phases and the intensities of reflections of both phases are in accordance with their initial compositions.

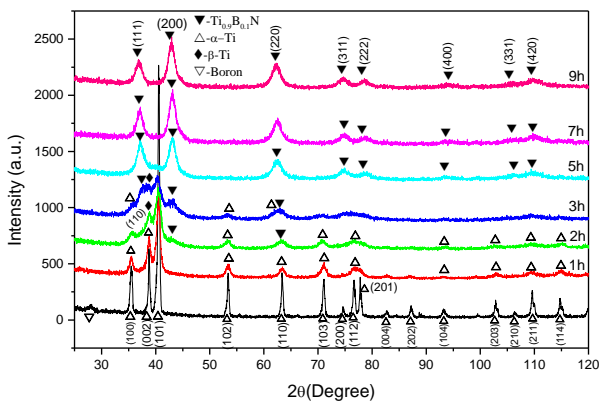


Fig.1. XRD patterns of unmilled and ball milled α -Ti and boron mixture under N_2 for different milling time.

It is very interesting to note that all B reflections disappear completely after 1h of milling. Peak broadening of α -Ti reflections increases continuously with increasing milling time which indicates that all B atoms are diffused into α -Ti lattice and a α -Ti based $0.9\text{Ti}-0.1\text{B}$ substitutional solid solution is formed after 1h of milling. As a result a small amount of cubic $\text{Ti}(\text{B},\text{N})$ phase similar to cubic TiN phase (ICSD CC 152807) is noticed to form from the α -Ti based TiB interstitial solid solution. The observed peak broadening in the TiB solid solution may be attributed

for small crystalline size and lattice strain developed inside the lattice due to fracture and re-welding mechanism during ball-milling. The small crystalline size enhances the probability of diffusion of nitrogen in the TiB solid solution to form cubic TiBN phase. After 2h of $\text{Ti}_{0.9}\text{B}_{0.1}\text{N}$ phase appears clearly with its most intense (200) reflections with significant peak broaden and peak overlapping with α -Ti reflections. After 7h of milling, $\text{Ti}_{0.9}\text{B}_{0.1}\text{N}$ phase is formed completely with the appearance of all its reflections. It is interesting to note that a part of α -Ti (hcp) phase transformed to short-lived β -Ti (cubic) phase after 1h of milling and survive upto 3h of milling. It may be noted that there is no isolated reflection of β -Ti phase in the XRD patterns but the (110) reflection of β -Ti phase is completely overlapped with the 2nd major (111) reflection of $\text{Ti}_{0.9}\text{B}_{0.1}\text{N}$ phase and as a result, the (111) reflection appears as the strongest reflection instead of (200) reflection. The existence of β -Ti (cubic) phase identified during Rietveld's structure

refinement process of XRD patterns which gives best fitting quality when the existence of β -Ti (cubic) phase is taken into account during analysis. The existence of β -Ti phase was also noticed during synthesis of nanocrystalline TiN phases by the same method of preparation [7].

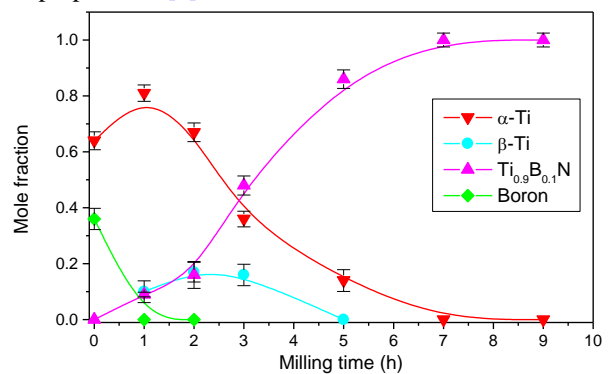


Fig.2. Variation of phase content (mol fraction) of different phases with increasing milling time.

The relative phase content of different phases of all unmilled and ball-milled sample are shown in Fig.2. The abundance of α -Ti and B phase in the unmilled sample is 0.64 and 0.36 mol fraction respectively, according to Rietveld's analysis though they mixed in 0.9: 0.1 molar ratio. This is because, the light weight boron powder covers more surface area than α -Ti powder during sample mounting in the XRD sample holder which in turn increases the relative peak area of the reflections of boron in the XRD pattern. After 1h of milling the content of boron phase become zero where as that α -Ti phase increases to 0.8 mol fraction. This indicates that all the boron atoms completely diffused to form TiB interstitial solid solution. Beside

this, significant amounts of α -Ti-phase transform partly to metastable cubic β -Ti phase (~0.1 mol fraction) after 1h and survive up to 3h of milling. During this time $Ti_{0.9}B_{0.1}N$ start to grow and the stoichiometric $Ti_{0.9}B_{0.1}N$ phase has been formed completely after 7h of milling.

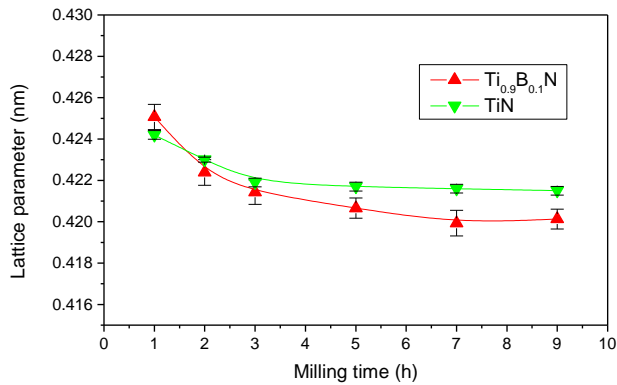


Fig. 3. Variation of lattice parameters of $(Ti_{0.9}B_{0.1})N$, TiN and β -Ti phases with increasing milling time.

At the very outset the cubic lattice parameter of TiBN phase (Fig. 3) formed with significantly greater value than that of TiN phase [7]. After 1h of milling the lattice parameter of cubic TiBN phase reduces continuously like TiN phase and continues to 2h of milling. The significant reduction of lattice parameter of TiBN phase with respect to TiN phase indicates the diffusion of boron atoms in α -Ti lattice. As there are no boron atoms left after 2h of milling the reduction lattice parameter of TiBN phase may be caused for (i) cold-working caused due to high impulsive collision force on $(Ti,B)N$ lattice during milling, (ii) to achieve a stable atomic configuration, constant re-arrangement of Ti and B atomic positions inside the lattice due to continuous diffusion of smaller N (ionic radius = 0.13Å) atoms.

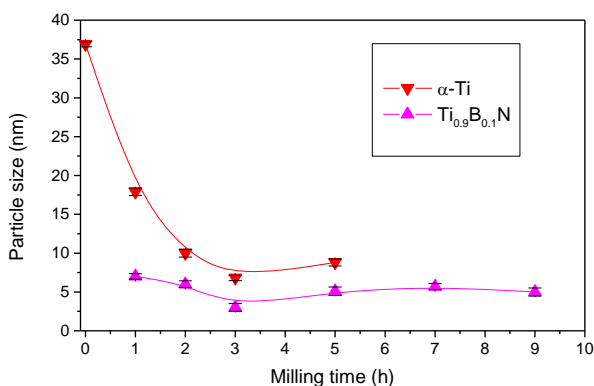


Fig.4. Variations of particle size of different phases with increasing milling time.

The variations of particle size of different phases are shown in the Fig. 4. The average particle size of α -Ti

phase reduces from ~37nm to ~18nm within 1h of milling when the formation of $(Ti,B)N$ phase is found to be initiated with particle size of ~7nm. After 3h of milling the particle size of α -Ti phase reduces rapidly to ~ 7nm and then it slightly increases to ~ 9nm after 5h of milling. Within 3h of milling the particle size of $(Ti,B)N$ phase decreases to ~ 3nm. This implies that addition of small amount of boron has great influence in reducing the size of $(Ti,B)N$ particles. It is interesting to note that in the course of milling up to 9h the particle size of $(Ti,B)N$ phase slightly increase to 5nm, due to agglomeration of smaller grains.

4.2 Nanostructure characterization by TEM

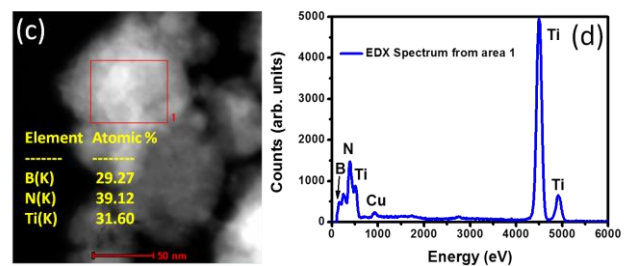


Fig. 5(c) & (d). Energy Dispersive X-ray (EDX) spectrum reveals the presence of Ti, B and N in the 9h milled $(Ti_{0.9}B_{0.1})N$ sample.

The elemental composition of 9h milled sample has been made by EDX analysis and is shown in Fig. 5(d). The high-angle annular dark-field scanning transmission electron microscopy (STEM-HAADF) image in Fig. 5(c) shows the sample position from where the EDX spectrum was collected. The EDX spectrum shows the relative intensities as well as relative abundance of elemental (Ti, B and N) compositions in 9h milled sample of $(Ti_{0.9}B_{0.1})N$. The details composition of the elements in the prepared sample is shown in the inset table of Fig. 5(c). Carbon and Cu peaks in EDX spectra are due to carbon coated copper grid used for TEM study.

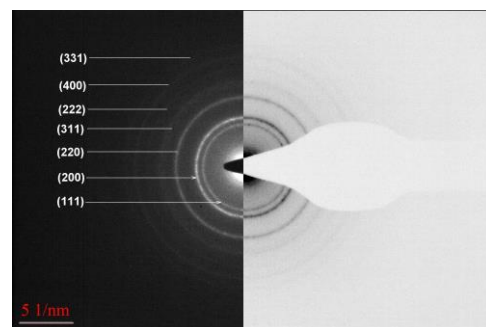


Fig.6. Selected area electron diffraction (SAED) pattern of nanocrystalline $(Ti_{0.9}B_{0.1})N$ powder after 9h of milling.

The selected area electron diffraction (SAED) pattern of 9h milled sample confirms the formation of (Ti,B)N phase (Fig.6). Like the XRD pattern, intense lines are well resolved though they are sufficiently broadened due to small particle size. As there is no trace of any other reflections in the SAED pattern, contaminations either from elemental powders or from milling media can be easily ruled out.

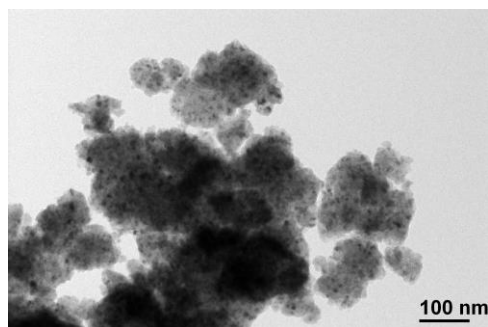


Fig. 7. TEM image of 9h ball-milled powder of $Ti_{0.9}B_{0.1}N$ nanoparticles.

The TEM image (Fig. 7) 9h ball-milled powder sample of $Ti_{0.9}B_{0.1}N$ shows that the average size of nanoparticles is ~ 5 nm. The nanoparticles are spherical in shape and are almost mono-dispersed with size lying between 2 -10 nm.

5. CONCLUSIONS

Stoichiometric nanocrystalline single phase ($Ti_{0.9}B_{0.1}N$) powders have been synthesized by mechanically alloying the elemental powder mixture of α -Ti and B under nitrogen atmosphere. Towards the formation of nanocrystalline ($Ti_{0.9}B_{0.1}N$) phase, the following important findings have been observed:

- i) Cubic ($Ti_{0.9}B_{0.1}N$) phase starts to form after 1h of milling and it formed completely after 7h of milling. An addition of 0.1 mol fraction of boron accelerates the formation time of ternary (Ti,B)N by 2 h in comparison to binary TiN.
- ii) Transient cubic β -Ti phase (bcc) is formed during milling.
- iii) Microstructure analysis of 9h milled sample both by Rietveld method and by HRTEM micrograph reveals that (Ti,B)N nanoparticles are almost mono-dispersed and their average particle size reduces to ~ 5 nm.
- iv) SAED pattern confirms the formation of good quality nanocrystalline ($Ti_{0.9}B_{0.1}N$) powder without any contamination.

6. ACKNOWLEDGEMENT

The author wish to thank to the University Grants Commission (UGC), India to grant UGC-MRP (Minor Research Project) and to Prof. S. K. Pradhan, Department of Physics, The University of Burdwan

for his motivation and support. The author is also grateful to SINP, Kolkata for providing the HRTEM facility.

REFERENCES

- [1] R.F. Bunshah (Ed.), Noyes Publications, New York, 2001.
- [2] C. Gautier, J. Machet, Thin Solid Films, 295 (1997) pp. 43-52.
- [3] Y.L. Su, S.H. Yao, Wear, 205 (1997), pp.112-119.
- [4] J.D. Demaree, C.G. Fountzoulas, J.K. Hirvonen, Surf. Coat. Technol., 86-87 (1996) pp.309-315.
- [5] B. Matthes, E. Broszeit, K.H. Kloos, Surf. Coat. Technol., 57 (1993) pp.97-104.
- [6] O. Knotek, R. Breidenbach, F. Jungblut, F. Loffler, Surf. Coat. Technol., 43-44 (1990) pp.107-115.
- [7] U.K. Bhaskar, S. Bid, B. Satpati, S.K. Pradhan, J. Alloys Compd., 493 (2010) pp. 192-196.
- [8] L. Lutterotti, P. Scardi, P. Maistrelli, J. Appl. Cryst., 25 (1992) pp. 459-462.
- [9] L. Lutterotti, MAU Dversion 2.55, (2015).<http://www.ing.unitn.it/~luttero/maud>.
- [10] H.M. Rietveld, Acta Cryst., 22 (1967) pp. 151-152.
- [11] H.M. Rietveld, J. Appl. Cryst., 2 (1969) pp. 65-71.
- [12] H. Toraya, J. Appl. Cryst., 33 (2000) pp. 1324-1328.
- [13] B.E. Warren, X-ray Diffraction, Chap. 13, Addison-Wesley, Reading, (1969).
- [14] D.B. Wiles, R.A. Young, J. Appl. Cryst., 14 (1981) pp. 149-151.
- [15] R.A. Young, D.B. Wiles, J. Appl. Cryst., 15 (1982) pp. 430-438.
- [16] R.A. Young, "The Rietveld Method", edited by R.A. Young, pp. 1-38, Oxford University Press /IUCr, 1996.